Journal of Agricultural Science and Technology B 2 (2012) 1203-1213
Earlier title: Journal of Agricultural Science and Technology, ISSN 1939-1250

Importance of a Well-distributed Frequency of Measurements in the Senescence Monitoring of Winter Wheat and Yield Estimates

Louis Kouadio, Bakary Djaby, Moussa El Jarroudi and Bernard Tychon

Department of Environmental Sciences and Management, University of Liege, Arlon Campus Environnement, Arlon 6700, Belgium

Received: August 24, 2012 / Published: December 20, 2012.

Abstract: Theoretical frequencies of green area index (GAI) measurements were assessed in order to bring out the optimum frequencies for the monitoring of the senescence of winter wheat as well as the relationships between metrics which could be derived and the final grain yield. Several profiles of GAI decreasing curves were elaborated based on field measurements. Two functions, usually employed in green leaf area decreasing curves fitting (i.e., modified Gompertz and logistic functions) were then used to characterize the senescence phase and to calculate their metrics. These analyses showed that the two curve fitting functions satisfactorily described the senescence phase on frequencies of four to six GAI measurements, well distributed throughout a period of 30-35 days. The regression-based modeling showed that those involving metrics from logistic function (i.e., maximum value of GAI, green area duration and senescent rate) were more suitable than that of the modified Gompertz function for wheat yield estimates. Such results could be useful for studies at larger scales (involving remote sensing airplane or satellite data) and focused on the senescence in terms of optimum number of measurements and frequencies for developing models for yield estimates.

Key words: Green area index, senescence, logistic function, yield, wheat.

1. Introduction

Growth and duration of green leaf area of a crop determine the percentage of the incident solar radiation that will be intercepted by the crop canopy across time, thereby influencing canopy photosynthesis, photosynthate translocation and final yield [1]. The total leaf area of a canopy is often quantified by a dimensionless variable called leaf area index (LAI), defined as half the total developed area of leaves per unit of ground horizontal surface area [2]. Many methods of LAI measurements have been reported [3-5] and vary greatly in their accuracy, bias and ease of measurement. LAI can be measured either directly (destructive approaches) or indirectly (non destructive approaches). The latter generally use optical sensors and are based on light transmittance or on canopy gap fraction measurements. The gap fraction is the probability of a light ray missing all foliage elements while passing through the canopy [6]. Because of the sensitivity of the gap fraction to both green and non-green vegetation elements, Baret et al. [7] have shown how green area index (GAI), rather than LAI or plant area index, was closer to the variable that could be estimated from gap fraction on the field. GAI, relating to the photosynthetically active (green) plant area with no differences between leaves, stems and reproductive organs, has been widely used in photosynthesis [8], canopy light interception [9, 10] and light use efficiency [11] in crop models because it is more closely related with the fraction of absorbed photosynthetically active radiation. Indirect determination of GAI requires optical devices able to separate green from senescent

Corresponding author: Louis Kouadio, Ph.D., research fields: agrometeorology and crop modeling. E-mail: al.kouadio@doct.ulg.ac.be.

or wooden parts within the canopy [4]. Among these devices, digital hemispherical photography became recently very popular since a large number of very high resolution images can be acquired with simple commercial cameras and next processed easily with most current computers [7]. Hemispherical photography is a technique for studying plant canopies via photographs acquired through a hemispherical (fisheye) lens from beneath the canopy (oriented towards zenith) or placed above the canopy looking downward [4]. However, a daily monitoring of crop canopy growth at field level, specifically the decline of its green area, remains expensive, laborious and time consuming.

In a previous study [12], we demonstrated that winter wheat (*Triticum aestivum* L.) yield can be estimated from metrics derived from the decreasing part of the GAI at field level. Although, this previous study gave interesting results on the senescence characterization and final yield estimates, the optimum number of GAI measurements has not been extensively studied. Moreover, in order to implement such methods in a large-scale monitoring framework, a good knowledge relating to the optimum number of measurements is of great interest. The present paper serves as an extension with additional analyses according to different frequencies of GAI measurements and its influence on: (1) the characterization of the senescence phase and (2) the performances of regression-based models for yield estimation. Based on field measurements of winter wheat GAI, different measurements frequencies were set up first. Characterizations of the senescence phase, as well as the calculation of metrics, were then performed through the curve fitting of GAI profiles using the modified Gompertz and logistic functions [13]. Finally, attention was paid to the regression-based models that could be assessed for yield estimates, and the usefulness of these findings for studies implying remote sensing (airborne or satellite) data.

2. Material and Methods

2.1 Field Data

Field experiments were carried out during the 2008-2009 cropping season in three sites in Luxembourg: Everlange (49°47′N, 5°57′E), Christnach (49°45′N, 6°14′E) and Burmerange (49°29′N, 6°19′E). Crop practices (sowing and harvest methods, weed control, fungicide treatment) were representative of usual wheat production in Luxembourg [14]. At each site, the wheat cultivar was sown in a randomized block design with four replicates. Each plot size was 8 m × 1.5 m and each replicate block consisted of treated (including double and triple fungicide treatment) or untreated (no fungicide treatment) plots. The fungicide treatment was always a mix of strobilurin and triazol.

Field GAI data were retrieved from digital hemispherical photography (DHP) taken above the canopy during the beginning of May and the beginning of July 2009 (Table 1). GAI values were determined by processing these DHP using the CAN-EYE [1] software (version 6.2). A description of the CAN-EYE software and its underlying equations is given by Weiss [5] and Demarez [15]. Due to the plot size, three DHP were taken above the canopy of each plot, with a spatial sampling of 1.5 m between DHP. Measurements were done at a height of approximately 0.7-1.0 m. The calculation of GAI value for each level of fungicide treatment was consequently achieved using the total DHP by level of treatment, that is to say 12 DHP. Canopies were relatively homogeneous throughout plots for a given level of fungicide treatment. This allowed gathering all DHP for the calculation of its corresponding GAI value.

2.2 Theoretical Frequencies of GAI Measurements

Theoretical frequencies of measurements based on field GAI data were then established. The period of measurements spanned approximately over 32 days at

[1] https://www4.paca.inra.fr/can-eye.

Table 1 Classes of combinations based on data of GAI available during the senescence phase GS : growing stage, phenological stage according to Zadoks scale [16]. DoY: Day of year.

	GS	DoY	With 4 values						With 5 values						With six values		With seven values
			C_41	C_42	C_43	C_44	C_45	C_46	C_51	C_52	C_53	C_54	C_55	C_56	C_61	C_62	C_7
Burmerange	61	153	X	X	X	X	X	X	X	X	X	X	X	X	X	X	X
	69	159	X	X	X	X			X	X	X	X			X	X	X
	69	163	X	X	X	X		X	X	X	X		X		X	X	X
	73	173	X					X	X	X	X			X	X	X	X
	77	177		X			X		X			X	X	X	X	X	X
	82	180			X		X			X		X	X	X	X		X
	83	184				X	X	X			X	X	X	X		X	X
Christnach	65	159	X	X	X	X	X	X	X	X	X	X	X	X	X	X	X
	69	163	X	X	X	X			X	X	X	X			X	X	X
	75	173	X	X	X	X		X	X	X	X		X		X	X	X
	77	177	X						X	X	X			X	X	X	X
	79	180		X			X	X	X			X	X	X	X	X	X
	83	184			X		X			X		X	X	X	X		X
	85	187				X	X	X			X	X	X	X		X	X
Everlange	65	159	X	X	X	X	X	X	X	X	X	X	X	X	X	X	X
	69	163	X	X	X	X			X	X	X	X			X	X	X
	72	173	X	X	X	X		X	X	X	X		X		X	X	X
	77	177	X						X	X	X			X	X	X	X
	79	180		X			X	X	X			X	X	X	X	X	X
	83	184			X		X			X		X	X	X	X		X
	85	187				X	X	X			X	X	X	X		X	X

Burmerange site, and 35 days at Christnach and Everlange sites. Seven GAI measurements have been done over this period for all sites. Four classes of combinations (class with four, five, six and seven values) were therefore elaborated, with at least four GAI values in each class (Table 1). Thus, the classes of combinations with four or five values (i.e., C_41 to C_44, C_51 to C_53) were characterized on the one hand by combinations with three or four GAI measurements in the first 10 days after the maximum GAI value, between growing stage GS 61 and GS 69 [16], and one GAI measurement in the two last weeks of measurements. On the other hand, these classes included combinations with three GAI measurements in the last two weeks and one or two measurements in the first half of the period of measurements (i.e., C_46, C_54 to C_56). Combinations with six GAI measurements differed only on the date of the final measurement considered, while the combination with seven values (C_7) was that with all data of GAI measured. Each combination was composed by nine values of GAI, representing three plots by three sites.

2.3 Characterizing the Senescence Phase of Green Area

The modified Gompertz (Eq. 1) and logistic (Eq. 2) functions [13] were chosen to describe the senescent phase in this study. Their formulae are given as follows:

$$GAI(t) = GAI_{\max} \cdot \exp\left[-\exp\left(-k\left(t-m\right)\right)\right] \quad (1)$$

$$GAI(t) = \frac{GAI_{\max}}{1+\left[\exp\left(-k\left(t-m\right)\right)\right]} \quad (2)$$

Where GAI_{max} refers to the maximum value of GAI, m is the position of the inflection point in the decreasing part of the GAI curve, k is the relative senescence rate,

and t is the thermal time expressed in growing degree-days.

The duration of green area during the senescence phase is expressed by the metric m. In Eq. 1 it corresponds to the thermal time taken to reach 37% (50% in Eq. 2) of green area remaining.

The quality of curve fitting was assessed through the variance accounted for (VAF) using these functions, the mean absolute error (MAE) and the root mean square error (RMSE). The corresponding formulae of these indicators are given in Table 2.

2.4 Relationship between Metrics of the Senescence Phase and Observed Yields

Results from multiple linear regressions were used to assess the relationships between metrics characterizing the senescence phase and observed yields. Multiple linear regressions were done separately by set of inputs according to each curve fitting function from which metrics are derived (Table 3).

To test the robustness and the ability of the generated regression-based models to estimate wheat grain yield at field level, a leave-one-out cross validation was performed. Statistics indicators (RMSE, MAE, relative RMSE [RRMSE], adjusted R^2 [adj. R^2]) were used to quantify the performances of these models (Table 2).

3. Results and Discussion

3.1 Curve Fitting of GAI Profiles

Globally, at least 85% of total combinations had a VAF value greater than 90%, regardless of the curve fitting function. The mean VAF value for the class combination with four and five GAI measurements varied between 85% and 99%, and between 93% and 98% for the class combination with six and seven GAI measurements. RMSE were low and ranging between 0.1 and 0.3 m^2 m^{-2} on average in all class combinations, suggesting a good fit. We can therefore report that the two curve fitting functions satisfactorily describe the senescence phase. Nonetheless, some differences between these functions were noted in the quality of their fitting. Comparing results of the two curve-fitting functions, out of 135 combinations, there were 93 where VAF using the logistic function was greater than those obtained using the modified Gompertz function. Similarly, in the case of MAE (or RMSE), there were 64% of combinations with MAE

Table 2 Statistics indicators and their definition.

Statistic	Formula
Variance accounted for	$VAF = 100\times\left(1-\frac{variance\ of\ residuals}{variance\ of\ observed\ values}\right)$
Mean absolute error	$MAE=\frac{1}{n}\sum_{i=1}^{n}\lvert E_i-O_i\rvert$
Root mean square error	$RMSE=\sqrt{\frac{SSE}{n-p}}$
Adjusted R^2	$adj.\ R^2=1-\frac{(n-1)(1-R^2)}{n-p}$
Relative root mean square error	$RRMSE=100\times\frac{RMSE}{\bar{O}}$

SSE: sum of squared errors; *E*: estimated yields; *O*: observed yields; $\bar{O}$: mean value of the observed yields; *n:* number of observations; *p:* number of parameters in the model.

Table 3 Parameters of models.

Model	Parameters of model	
	Modified Gompertz function	Logistic function
Mod. 1	m_{gomp}, GAI_{max}	m_{log}, GAI_{max}
Mod. 2	k_{gomp}, GAI_{max}	k_{log}, GAI_{max}
Mod. 3	m_{gomp}, k_{gomp}	m_{log}, k_{log}
Mod. 4	m_{gomp}, k_{gomp}, GAI_{max}	m_{log}, k_{log}, GAI_{max}

obtained after fitting by the modified Gompertz function greater than those obtained after fitting by the logistic function. The ANOVA performed with the VAF and the MAE revealed that they were significantly different ($P < 0.01$ in case of the VAF and $P < 0.05$ in case of MAE). The statistical difference between the results of the curve fitting functions on the one hand, and the number of good fitting by the logistic function on the other hand, therefore, showed that this latter should be preferred to characterize the senescent phase of winter wheat GAI at the field level.

3.2 Frequency of GAI Measurements and Characterization of the Senescence Phase

Each combination studied refers to one theoretical frequency of GAI measurement. The mean MAE values were almost the same within each class of combination. These values were low and ranging between 0.02 and 0.29 m^2 m^{-2}, for the two curve-fitting functions for all the combinations. The mean VAF values increased from the first to the last in each class of combination (e.g., class with four, five and six GAI measurements, Fig. 1). Low mean VAF values were associated to combinations C_41, C_42, C_51 and C_52 (Fig. 1). These combinations involved either three, four or five GAI measurements in the first 10 to 20 days following GAI_{max} (Table 1). The GAI measurements in these combinations were not well distributed throughout the senescence phase. The period of measurements spanned approximately over 32 days for Burmerange site and 35 days for both Christnach and Everlange sites. All the GAI values in the combinations above were ranged between GAI_{max} and the end of milky ripening growth stage (Table 1). Adding one or two GAI measurements after the first 20 days following GAI_{max}, along with a well-distributed frequency, gave a better description of the senescence phase (mean VAF greater than 90%, Fig. 1). A good characterization of the decreasing phase is one which associates high VAF value and low MAE value. In such a case, comparing the mean VAF and MAE values, combinations with satisfactory characteristics were the last three in class combination with four measurements (C_44 and C_46): the mean VAF was greater than 95% (Fig. 1) and a mean MAE not greater than 0.15 m^2 m^{-2} (Fig. 2). Results of combinations C_55, C_56 and C_62 were quite similar to these results.

Data available in this study allowed two classes of combination with six measurements and one class with seven measurements. This made comparisons with other classes difficult. Nonetheless, despite its seven measurements during the senescence phase, the combination C_7 presented low VAF values and high MAE value on average, compared to the best classes in combinations with four and five measurements (C_44-C_46 and C_55-C_56, Fig. 1 and Fig. 2). This could be explained by GAI values which appeared as "outlier" in the decreasing phase. An example of curve fitting with "outlier" is shown in Fig. 3. Statistical indicators of the second curve fitting (Fig. 3b) are more interesting than those of the first (Fig. 3a). In this latter, the second GAI value after the GAI_{max} tends to increase the MAE and to reduce the VAF. The fungicide treatments involved in each site allowed different decreasing phases of the GAI. The distribution of VAF by fungicide treatment shows that three low VAF values were associated to plots with two fungicide treatments. In these cases, the curve-fitting functions did not suit well to GAI profiles. There is no physiological assumption explaining this fact. These bad characterizations appeared in profiles where some GAI values seem to be "outlier". GAI measurements are sensitive to a range of external and internal factors, often inducing difficult-to-define errors in the final estimate at the scale of interest. Such GAI values might be accounted for by differences in photographic exposure (e.g., presence of wind, boundary effects) despite every care being taken to make these as similar as possible. The number of bad curve fitting did not however disturb

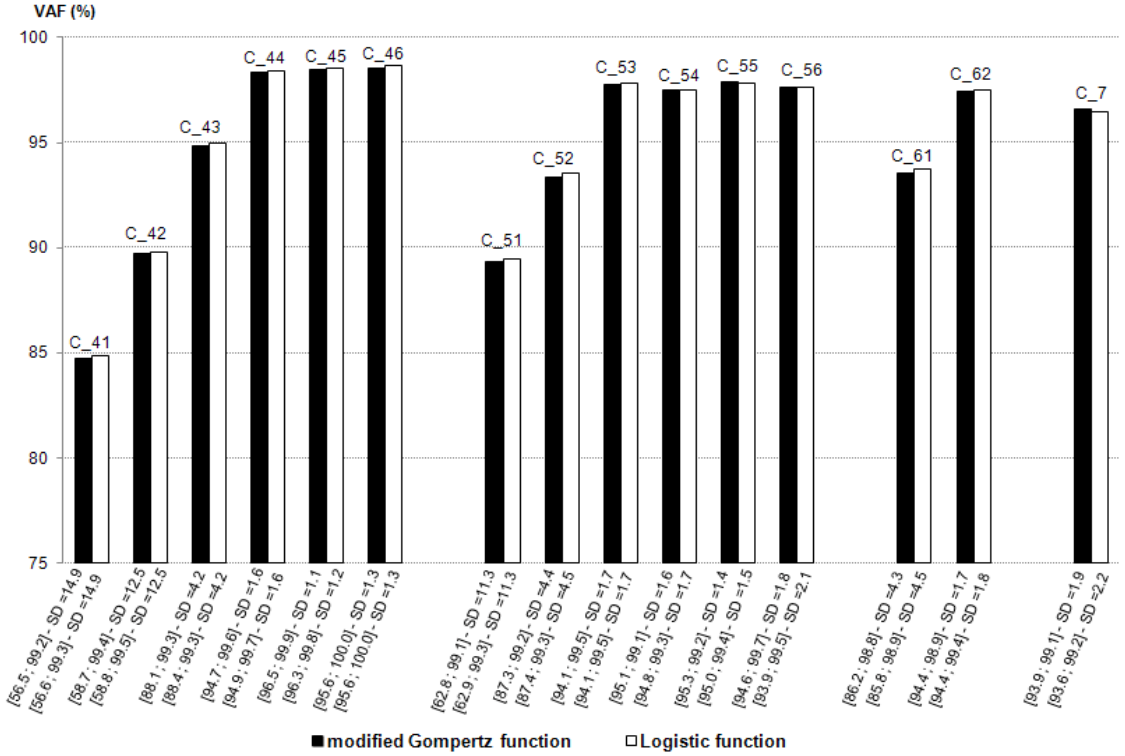

Fig. 1 Average VAF value by curve fitting function and combination. Numbers in brackets express the range of VAF for the combination. SD designs the standard deviation.

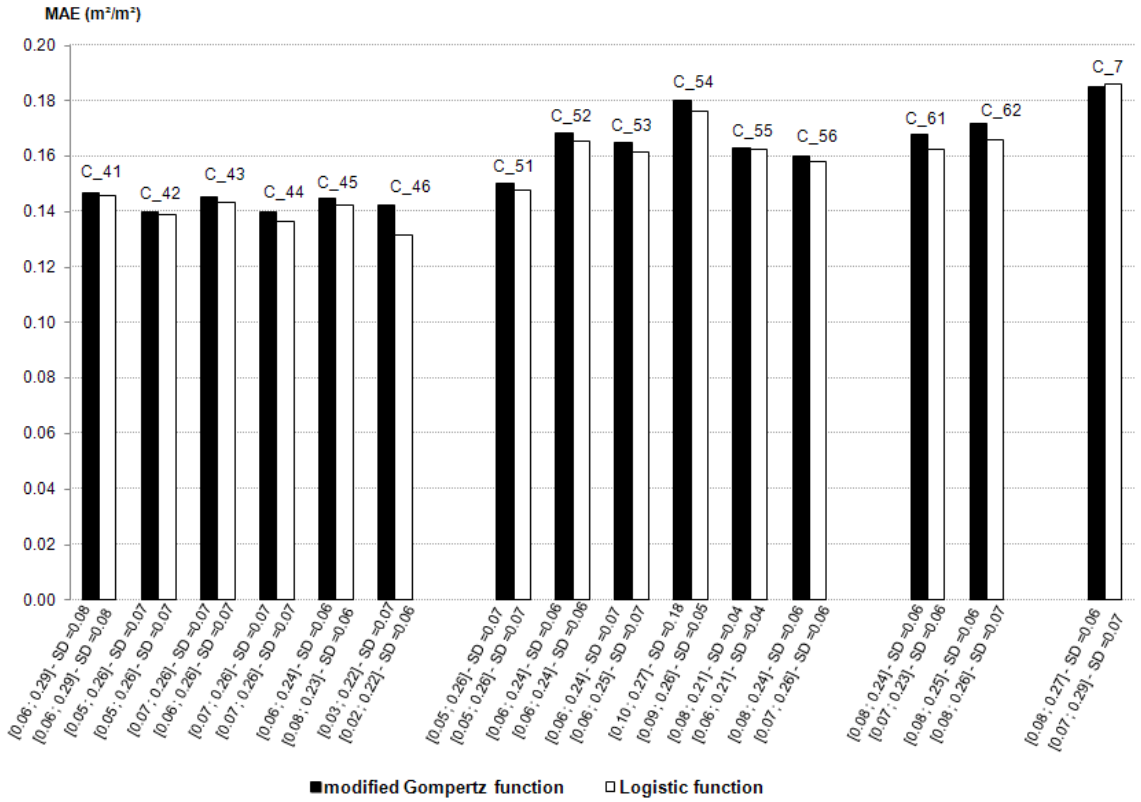

Fig. 2 Average MAE value by curve fitting function and by combination. Numbers in brackets express the range of VAF for the combination. SD designs the standard deviation.

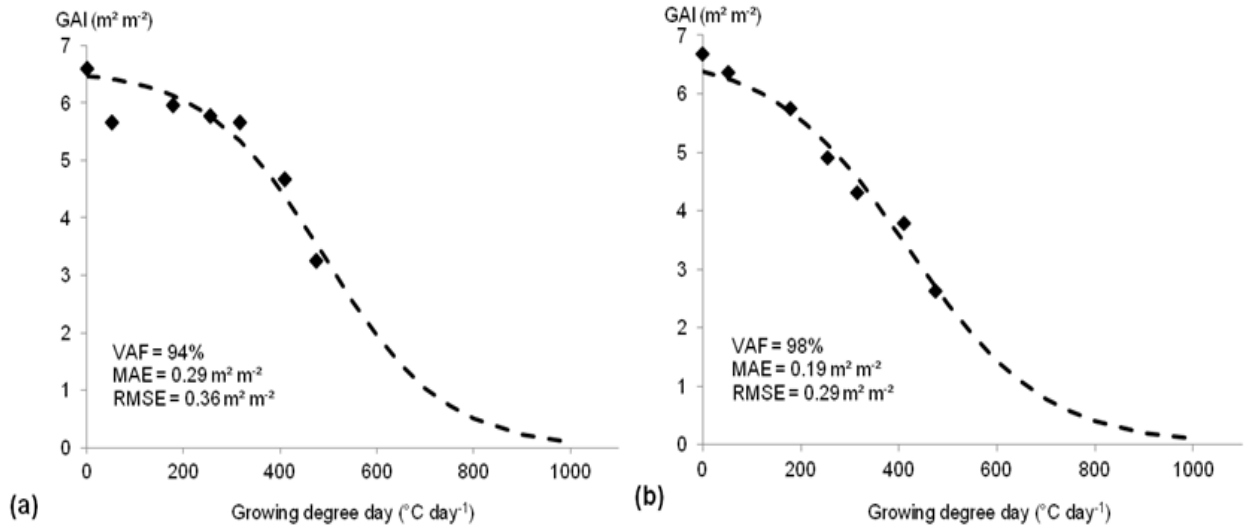

Fig. 3 Curve-fitting of two different GAI profiles in class combination with seven measurements (logistic function). (a) Plot with two fungicide treatments; (b) Plot with no fungicide treatment. The dashed line represents the adjusted curve. The points are the measured values of GAI.

the overall goodness of fitting. In order to assess the relationships between metrics and yield in the subsequent analyses, metrics derived from fitting with VAF greater than or equal to 80% were taken into account.

3.3 Relationships between Metrics and Grain Yield

Results of models assessed by combination along with their performances criteria are shown in Table 4 and Table 5. Generally, for all combinations, the model Mod. 2 (involving the senescence rate and GAI_{max}) did not explain significantly the variability in observed yields, regardless the curve-fitting function from which metrics were derived. Non statistical significativity was also observed in the case of combinations C_41, C_42, C_43, C_51, C_52 and C_61 according to models Mod. 1, Mod. 3 and Mod. 4. The non-significant models were associated to combinations with bad curve-fitting characteristics. For the other combinations, regression-based models were statistically significant and the adj. R^2 greater than 0.75 (Tables 4 and 5). The adj. R^2 and the MAE varied between 0.75 and 0.84 and between 0.42 and 0.51 t ha^{-1}, respectively, according to models involving metrics from the modified Gompertz function (Table 4). For models involving metrics from the logistic function, the adj. R^2 ranged between 0.82 and 0.88, and the MAE between 0.33 and 0.40 t ha^{-1}. Models with high level of significance were those involving metrics from the logistic function (C_44, C_46, C_53 and C_62, Table 5). The corresponding RMSE of the three models Mod. 1, Mod. 3 and Mod. 4 for these combinations varied between 0.35 and 0.49 t ha^{-1}; whereas the range of the RMSE of models with metrics from Gompertz function was between 0.45 and 0.58 t ha^{-1} (Tables 4 and 5). Given the statistical indicators obtained with models of the combination with all GAI measurements (i.e., C_7: adj. R^2 ranged between 0.81 and 0.87 and RMSE ranged between 0.38 and 0.50 t ha^{-1}), models with interesting characteristics could be obtained in combinations with four to six GAI values. These conclusions are confirmed through the validation phase performed on statistically significant models.

The results of the cross-validation of significant models for each combination are shown in Table 6. The RMSE of models were less than 0.62 t ha^{-1} and ranging between 0.44 and 0.62 t ha^{-1} for models based on metrics derived from modified Gompertz function, while for that of the logistic function this range was between 0.42 and 0.54 t ha^{-1} (Table 6). According to GAI data available in this study, these results showed

Table 4 Statistical test results for yield estimates (models based on metrics derived from the modified Gompertz function).

	Mod. 1				Mod. 2				Mod. 3				Mod. 4			
Parameters	m_{gomp}, GAI_{max}				k_{gomp}, GAI_{max}				m_{gomp}, k_{gomp}				m_{gomp}, k_{gomp}, GAI_{max}			
	adj. R^2	MAE (t ha^{-1})	RMSE (t ha^{-1})	Model significance ($P > F$)[a]	adj. R^2	MAE (t ha^{-1})	RMSE (t ha^{-1})	Model significance ($P > F$)[a]	adj. R^2	MAE (t ha^{-1})	RMSE (t ha^{-1})	Model significance ($P > F$)[a]	adj. R^2	MAE (t ha^{-1})	RMSE (t ha^{-1})	Model significance ($P > F$)[a]
C_41	-0.03	0.96	1.17	ns	-0.03	0.96	1.17	ns	-0.10	1.05	1.21	ns	-0.23	0.96	1.17	ns
C_42	-0.01	0.92	1.16	ns	-0.04	0.94	1.18	ns	-0.19	1.16	1.26	ns	-0.2	0.90	1.15	ns
C_43	0.43	0.73	0.87	ns	-0.03	0.91	1.13	ns	0.29	0.86	0.97	ns	0.48	0.61	0.76	ns
C_44	0.83	0.43	0.48	**	0.07	0.94	1.11	ns	0.8	0.45	0.51	**	0.79	0.43	0.47	*
C_45	0.75	0.51	0.58	**	-0.08	0.90	1.20	ns	0.76	0.48	0.57	**	0.71	0.48	0.57	*
C_46	0.84	0.42	0.46	**	0.03	0.90	1.14	ns	0.83	0.43	0.47	**	0.81	0.43	0.46	**
C_51	-0.01	0.93	1.16	ns	-0.06	0.95	1.19	ns	-0.24	1.22	1.28	ns	-0.15	0.85	1.13	ns
C_52	0.41	0.73	0.89	ns	0.00	0.93	1.15	ns	0.24	0.86	1.01	ns	0.59	0.53	0.68	ns
C_53	0.83	0.43	0.47	**	0.17	0.81	1.05	ns	0.83	0.43	0.48	**	0.80	0.43	0.47	*
C_54	0.81	0.46	0.50	**	-0.05	0.92	1.18	ns	0.78	0.49	0.54	**	0.79	0.44	0.48	*
C_55	0.81	0.46	0.51	**	-0.04	0.91	1.19	ns	0.78	0.48	0.54	**	0.77	0.44	0.50	*
C_56	0.84	0.42	0.47	**	-0.06	0.87		ns	0.84	0.42	0.47	**	0.8	0.42	0.47	*
C_61	0.42	0.74	0.88	ns	0.03	0.91	1.14	ns	0.19	0.89	1.04	ns	0.62	0.52	0.65	ns
C_62	0.84	0.43	0.46	**	0.16	0.88	1.06	ns	0.83	0.43	0.47	**	0.82	0.43	0.45	**
C_7	0.82	0.44	0.49	**	0.11	0.93	1.09	ns	0.81	0.45	0.50	**	0.82	0.41	0.45	**

[a]P value associated with F value (this ratio compares variability explained by the regression line with variability not explained by the regression line). Significant level, *$P < 0.05$; **$P < 0.01$ and ns: $P > 0.05$.

Table 5 Statistical test results for yield estimates (models based on metrics derived from the logistic function).

	Mod.1				Mod.2				Mod.3				Mod.4			
Parameters	m_{loo}, GAI_{max}				k_{log}, GAI_{max}				m_{log}, k_{log}				m_{log}, k_{log}, GAI_{max}			
	adj. R^2	MAE (t ha^{-1})	RMSE (t ha^{-1})	Model significance ($P > F$)[a]	adj. R^2	MAE (t ha^{-1})	RMSE (t ha^{-1})	Model significance ($P > F$)[a]	adj. R^2	MAE (t ha^{-1})	RMSE (t ha^{-1})	Model significance ($P > F$)[a]	adj. R^2	MAE (t ha^{-1})	RMSE (t ha^{-1})	Model significance ($P > F$)[a]
C_41	-0.01	0.95	1.16	ns	-0.02	0.96	1.16	ns	-0.08	1.04	1.20	ns	-0.21	0.95	1.16	ns
C_42	0.02	0.91	1.14	ns	-0.01	0.94	1.16	ns	-0.16	1.14	1.24	ns	-0.18	0.90	1.14	ns
C_43	0.48	0.67	0.83	ns	0.1	0.91	1.09	ns	0.28	0.87	0.98	ns	0.48	0.62	0.76	ns
C_44	0.87	0.36	0.41	***	0.32	0.81	0.95	ns	0.88	0.34	0.40	***	0.89	0.30	0.35	**
C_45	0.82	0.42	0.49	**	-0.03	0.87	1.17	ns	0.82	0.43	0.49	**	0.79	0.44	0.49	*
C_46	0.88	0.33	0.40	***	0.24	0.84	1.01	ns	0.88	0.34	0.39	***	0.86	0.35	0.39	**
C_51	0.02	0.93	1.14	ns	-0.03	0.95	1.17	ns	-0.21	1.20	1.27	ns	-0.15	0.86	1.13	ns
C_52	0.46	0.70	0.85	ns	0.08	0.91	1.10	ns	0.21	0.87	1.02	ns	0.55	0.55	0.71	ns
C_53	0.87	0.36	0.41	***	0.61	0.58	0.72	*	0.87	0.36	0.41	***	0.87	0.35	0.39	**
C_54	0.84	0.40	0.46	**	0.06	0.92	1.12	ns	0.85	0.39	0.45	**	0.86	0.35	0.48	**
C_55	0.84	0.40	0.46	**	0.08	0.91	1.10	ns	0.85	0.39	0.44	**	0.84	0.37	0.42	**
C_56	0.86	0.35	0.44	**	0.06	0.83	1.12	ns	0.87	0.34	0.42	**	0.84	0.35	0.42	**
C_61	0.46	0.71	0.85	ns	0.12	0.91	1.08	ns	0.18	0.90	1.05	ns	0.56	0.57	0.70	ns
C_62	0.87	0.36	0.41	***	0.55	0.65	0.78	*	0.88	0.35	0.39	***	0.88	0.33	0.36	**
C_7	0.83	0.40	0.47	**	0.48	0.74	0.83	ns	0.86	0.38	0.44	**	0.87	0.34	0.38	**

[a]P value associated with F value (this ratio compares variability explained by the regression line to variability not explained by the regression line). Significant level. *$P < 0.05$; **$P < 0.01$; ***$P < 0.001$ and ns: $P > 0.05$.

that a number of four to six GAI measurements, well distributed throughout the senescence phase (one or two measurements in the first half of the period of measurements and three measurements in the last two weeks), could lead to satisfactory performances of models for yield estimation. Comparing models

Table 6 Models performances after the validation test (leave-one-out cross-validation). Only statistically significant models are shown in the table.

	Modified Gompertz function						Logistic function					
	Mod. 1		Mod. 3		Mod. 4		Mod. 1		Mod. 3		Mod. 4	
	RMSE (t ha^{-1})	MAE (t ha^{-1})	RMSE (t ha^{-1})	MAE (t ha^{-1})	RMSE (t ha^{-1})	MAE (t ha^{-1})	RMSE (t ha^{-1})	MAE (t ha^{-1})	RMSE (t ha^{-1})	MAE (t ha^{-1})	RMSE (t ha^{-1})	MAE (t ha^{-1})
C_44	0.51 (4)	0.44	0.56 (4)	0.46	0.56 (4)	0.45	0.44 (4)	0.37	0.43 (3)	0.36	0.41 (3)	0.33
C_45	0.61 (5)	0.51	0.61 (5)	0.49	0.62 (5)	0.50	0.52 (4)	0.43	0.52 (4)	0.43	0.54 (4)	0.44
C_46	0.49 (4)	0.43	0.51 (4)	0.43	0.53 (4)	0.43	0.42 (3)	0.34	0.43 (3)	0.35	0.44 (3)	0.35
C_53	0.51 (4)	0.44	0.44 (3)	0.44	0.52 (4)	0.44	0.44 (4)	0.37	0.44 (4)	0.37	0.43 (3)	0.36
C_54	0.53 (4)	0.47	0.48 (4)	0.50	0.54 (4)	0.45	0.49 (5)	0.41	0.48 (4)	0.40	0.45 (3)	0.36
C_55	0.54 (4)	0.47	0.48 (4)	0.49	0.58 (5)	0.46	0.49 (5)	0.40	0.48 (4)	0.39	0.47 (4)	0.38
C_56	0.49 (4)	0.43	0.45 (3)	0.43	0.53 (4)	0.43	0.46 (4)	0.36	0.45 (4)	0.35	0.48 (4)	0.37
C_62	0.49 (4)	0.43	0.51 (4)	0.44	0.51 (4)	0.43	0.44 (4)	0.37	0.42 (3)	0.36	0.42 (3)	0.34
C_7	0.52 (4)	0.44	0.54 (4)	0.46	0.50 (4)	0.41	0.50 (4)	0.41	0.47 (4)	0.39	0.42 (3)	0.35

[a]Numbers in brackets designed the RRMSE (expressed in %).

according to the curve-fitting function from which metrics were derived, this study also revealed good criteria of models involving metrics from the logistic function.

Theoretical frequencies of GAI measurements allowed a wide range of situations to be analysed. Absolute rules on applying, evaluating and choosing a function to fit a curve are difficult to establish because there are too many factors and purposes (explicative, descriptive or predictive purpose) involved in the fitting of a curve [17]. The choice of function will, therefore, depend on the specific purposes of the study, the compliance with expected and observed curve shapes and the purpose of comparing parameter values with those found in the literature. In our study the modified Gompertz and logistic functions were chosen to describe and characterize the decreasing phase of winter wheat GAI. The logistic function has been used in various studies to describe or to simulate the process of individual leaves senescence [18-20]. A key hypothesis underlying this study is that GAI_{max} was determined as a maximum value reached during field observations, and consequently depending on the initial experimental protocol [12]. Even though this initial experimental protocol was elaborated in order to minimize such errors in the determination of GAI_{max}, further research is needed to determine whether this determination could influence the characterization of the senescence phase and the performances of regression-based models.

The analyses carried out in this study are very interesting because they allow an identification of possible frequency of GAI measurements during the senescence phase which give a satisfactory estimation of grain yields. The regression-based models, involving the GAI_{max}, the senescence rate and the green area duration (expressed through the time to reach 50% or 37% of green area remaining), showed satisfactory performances for yield estimation: RMSE of about 0.35-0.49 t ha^{-1}, and 0.45 and 0.58 t ha^{-1} for models based on metrics derived from the logistic function and modified Gompertz function, respectively. Although the study is based on GAI calculated from hemispherical photography, it could be useful in researches based on data retrieved from air- or space-borne sensors in order (1) to characterize the shape of wheat senescence phase and (2) to relate its yield to metrics calculated from this phase. Providing crop-specific biophysical variables, such as GAI, at relevant spatial and temporal resolutions can help crop growth modelling improvement or simple approaches development/improvement for yield forecasting at national or regional scales. Remote sensing imagery can be acquired by a range of

airborne and space-borne sensors from multispectral sensors to hyperspectral sensors with wavelengths ranging from visible to microwave, spatial resolutions ranging from sub-metre to kilometre and temporal frequencies ranging from 30 min to weeks or months (XIE [21] for review). The amount of measurements in time could be limited, however, resulting in the absence of images at critical moments during the growing season. This study could therefore serve as a basis for further studies on the use of GAI temporal profiles retrieved from earth observation satellite data and focusing on the phase of senescence in winter wheat yield estimates.

4. Conclusions

The evolution of wheat canopy during the crop season, especially during the grain filling and maturation stages, is of great interest in the determination of grain yield. This paper sought to study the influence of wheat GAI measurements frequencies on the monitoring of the senescence and the estimation of yield. Based on field monitoring spanning over 30-35 days and theoretical frequencies of measurements, this study suggests that a number of four to six GAI measurements, well distributed throughout the senescence phase, could lead to a satisfactory description of its decreasing phase using a logistic function and acceptable models for yield estimation.

Acknowledgments

This study took place within the framework of the GLOBAM project (global agricultural monitoring systems by integration of earth observation and modelling techniques), funded by the Belgian Science Policy, and the MACRY project, funded by the Administration des Services Techniques de l'Agriculture of Luxembourg. The first author was funded by a Ph.D. grant provided by the Presidency of the Republic of Côte d'Ivoire. The authors are also grateful to Farid Traoré and Michel Noel for their technical support.

References

[1] R.F. Dale, D.T. Coelho, K.P. Gallo, Prediction of daily green leaf area index for corn, Agron. J. 72 (1980) 999-1005.

[2] J.M. Chen, T.A. Black, Defining leaf area index for non-flat leaves, Plant, Cell Environ. 15 (1992) 421-429.

[3] N.J.J. Bréda, Ground-based measurements of leaf area index: A review of methods, instruments and current controversies, J. Exp. Bot. 54 (2003) 2403-2417.

[4] I. Jonckheere, S. Fleck, K. Nackaerts, B. Muys, P. Coppin, M. Weiss, et al., Review of methods for in situ leaf area index determination Part I. Theories, sensors and hemispherical photography, Agric. For. Meteorol. 121 (2004) 19-35.

[5] M. Weiss, F. Baret, G.J. Smith, I. Jonckheere, P. Coppin, Review of methods for in situ leaf area index (LAI) determination Part II. Estimation of LAI, errors and sampling, Agric. For. Meteorol. 121 (2004) 37-53.

[6] S.T. Gower, C.J. Kucharik, J.M. Norman, Direct and indirect estimation of leaf area index, FAPAR, and net primary production of terrestrial ecosystems-a real or imaginary problem?, Remote Sens. Environ. 70 (1999) 29-51.

[7] F. Baret, B. de Solan, R. Lopez-Lozano, K. Ma, M. Weiss, GAI estimates of row crops from downward looking digital photos taken perpendicular to rows at 57.5° zenith angle: Theoretical considerations based on 3D architecture models and application to wheat crops, Agric. For. Meteorol. 150 (2010) 1393-1401.

[8] R. Leuning, F.X. Dunin, Y.P. Wang, A two-leaf model for canopy conductance, photosynthesis and partitioning of available energy. II. Comparison with measurements, Agric. For. Meteorol. 91 (1998) 113-125.

[9] B.D. Thomson, K.H.M. Siddique, Grain legume species in low rainfall Mediterranean-type environments II. Canopy development, radiation interception, and dry-matter production, Field Crops Res. 54 (1997) 189-199.

[10] M.J. Foulkes, R.K. Scott, R. Sylvester-Bradley, The ability of wheat cultivars to withstand drought in UK conditions: Resource capture, J. Agric. Sci. 137 (2001) 1-16.

[11] P.D. Jamieson, M.A. Semenov, Modelling nitrogen uptake and redistribution in wheat, Field Crops Res. 68 (2000) 21-29.

[12] L. Kouadio, B. Djaby, G. Duveiller, M. El Jarroudi, B. Tychon, Cinétique de décroissance de la surface verte et estimation du rendement du blé d'hiver, Biotechnol. Agron. Soc. Environ. 16 (2012) 179-191.

[13] M.J. Gooding, J.P.R.E. Dimmock, J. France, S.A. Jones, Green leaf area decline of wheat flag leaves: The influence of fungicides and relationships with mean grain

weight and grain yield, Ann. Appl. Biol. 136 (2000) 77-84.

[14] M. El Jarroudi, P. Delfosse, H. Maraite, L. Hoffmann, B. Tychon, Assessing the accuracy of simulation model for *Septoria* leaf blotch disease progress on winter wheat, Plant Dis. 93 (2009) 983-992.

[15] V. Demarez, S. Duthoit, F. Baret, M. Weiss, G. Dedieu, Estimation of leaf area and clumping indexes of crops with hemispherical photographs, Agric. For. Meteorol. 148 (2008) 644-655.

[16] J.C. Zadoks, T.T. Chang, C.F. Konzak, A decimal code for the growth stages of cereals, Weed Res. 14 (1974) 415-421.

[17] E. Tjørve, Shapes and functions of species-area curves (II): A review of new models and parameterizations, J. Biogeogr. 36 (2009) 1435-1445.

[18] D.W. Stewart, L.M. Dwyer, A model of expansion and senescence of individual leaves of field-grown maize (*Zea mays* L.), Can. J. Plant Sci. 74 (1994) 37-42.

[19] X. Yin, A.H.C.M. Schapendonk, M.J. Kropff, M. van Oijen, P.S. Bindraban, A generic equation for nitrogen-limited leaf area index and its application in crop growth models for predicting leaf senescence, Ann. Bot. 85 (2000) 579-585.

[20] J.I. Lizaso, W.D. Batchelor, M.E. Westgate, A leaf area model to simulate cultivar-specific expansion and senescence of maize leaves, Field Crops Res. 80 (2003) 1-17.

[21] Y. Xie, Z. Sha, M. Yu, Remote sensing imagery in vegetation mapping: A review, J. Plant Ecol. 1 (2008) 9-23.